Performance Analysis of Nonlinear Energy-Harvesting DF Relay System in Interference-Limited Nakagami-*m* Fading Environment

Aleksandra Cvetkovic (iD), Vesna Blagojevic, and Predrag Ivaniš

A decode-and-forward system with an energy-harvesting relay is analyzed for the case when an arbitrary number of independent interference signals affect the communication at both the relay and the destination nodes. The scenario in which the relay harvests energy from both the source and interference signals using a time switching scheme is analyzed. The analysis is performed for the interference-limited Nakagami-*m* fading environment, assuming a realistic nonlinearity for the electronic devices. The closed-form outage probability expression for the system with a nonlinear energy harvester is derived. An asymptotic expression valid for the case of a simpler linear harvesting model is also provided. The derived analytical results are corroborated by an independent simulation model. The impacts of the saturation threshold power, the energy-harvesting ratio, and the number and power of the interference signals on the system performance are analyzed.

Keywords: Decode-and-forward relay scheme, Interference-limited environment, Nakagami-*m* fading, Nonlinear energy harvesting, Outage probability.

I. Introduction

It is well-known that the use of cooperation provides an improvement in the performance, reliability, and coverage of wireless networks [1]. The ever-increasing number of devices in wireless networks calls for a fundamentally different approach for powering devices as traditional battery replacement becomes impractical and costly. The use of energy-harvesting techniques represents a promising solution to this problem and has attracted a considerable amount of attention from the scientific community in recent years [2]–[4].

Although natural energy sources offer ecological solutions, radio frequency (RF) energy harvesting provides a reliability that is of essential importance for this type of network. An energy-harvesting-based system in which a node is only powered by useful signal energy was analyzed in [5]–[7]. Although the co-channel interference (CCI) in traditional communication systems always deteriorates the system performance [8]–[10], the effect of interference in systems with energy harvesting is two-fold. Moreover, the interference signal jeopardizes communication, but it also serves as the energy source for the harvesting relay and therefore might improve the relay transmit power and system performance [11]. An analysis of a system that employs energy harvesting from both the useful and interference signals at the receiver is provided in [12], considering the optimal switching mode between information and power transfer for the point-to-point link. A performance analysis of a network where a transmitter device with multiple antennas harvests energy from interference and ambient RF sources is provided in [13]. Furthermore, analyses of networks with an energy-harvesting and interference alignment algorithm can be

found in [14], [15]. Finally, a novel cooperative mechanism with spectrum sharing and energy harvesting from both the useful and ambient signals was proposed for 5G networks in [16], as it simultaneously addresses the challenges of energy and spectral efficiency.

The concept of a decode-and-forward (DF) relay that harvests energy from both the source and CCI signals was proposed in [17] considering a Rayleigh fading environment. An analysis of the impact of the CCI on an amplify-and-forward (AF) relay network was later provided in [18]. However, both papers considered the linear energy harvester model, which might be impractical in realistic scenarios owing to the nonlinearities of the electronic components, as recently reported in [19], [20]. Analyses of AF and DF relaying networks with a nonlinear model were provided in [21] and [22], respectively. Still, these papers do not consider the impact of the CCI signals on the performance of the energy-harvesting relaying system.

In this paper, we analyze a system with a DF relay that harvests energy from both the source and CCI using a time switching scheme. In contrast to [17], a nonlinear model of energy harvesting at the relay is applied, where the harvested energy of the relay depends on both the input power and saturation threshold power. In the observed system, the interference signals are presented at both the relay and destination nodes, whereas in [17], the CCI disturbs communication only at the relay node. Additionally, a more general case of a Nakagami-m distributed fading environment is considered in our paper.

The main contributions of the paper are as follows:

- We analyze the nonlinear energy-harvesting DF relay system, where communication is affected by the existence of an arbitrary number of independent interference signals at both the relay and the destination nodes.
- We derive a novel exact closed-form expression for the outage probability of the interference-limited system and the general case of a Nakagami-m distributed fading environment, which accurately models a wide range of propagation scenarios. The impacts of the system and channel parameters on the system performance are demonstrated.
- Simple asymptotic expressions for the outage probability that are valid for important scenarios are derived, enabling a more simple analysis with a high accuracy.

The rest of the paper is organized as follows. Section II describes the system and channel model. In Section III, an outage probability analysis is presented with the corresponding derivations given in Appendices I and II.

Numerical and simulation results for the outage probability and throughput with discussions are presented in Section IV. Some concluding remarks are given in Section V.

II. System and Channel Model

We consider the DF relaying system model shown in Fig. 1, where the source node S communicates with the destination D via the DF relay R without a direct link between them. The source node transmits the signal s with the power P_S to the relay, and the signal at the relay node is subject to the simultaneous impact of N independent CCI signals. We consider the interference-limited scenario, where the power of the interference signals is much larger than the additive white Gaussian noise power at the relay and destination nodes; thus, the latter can be neglected in the analytical derivations, as in [8], [9].

Therefore, the received signal at the relay R is

$$y_{SR} = \sqrt{P_S}h_{SR}s + \sum_{i=1}^{N} \sqrt{P_{Ri}}g_{Ri}s_{Ri}, \qquad (1)$$

where the interference signal is denoted by s_{Ri} with the corresponding signal power of P_{Ri} ($i = 1, \dots, N$). Further, h_{SR} and g_{Ri} ($i = 1, \dots, N$) are the channel fading gains between S and R and from ith interference source to R, respectively.

On the basis of (1), the received signal-to-interference ratio (SIR) at the relay is defined as

$$\gamma_R = \frac{P_S|h_{SR}|^2}{\sum\limits_{i=1}^{N} P_{Ri}|g_{Ri}|^2} = \frac{\gamma_{SR}}{I_R}, \qquad (2)$$

where $\gamma_{SR} = P_S|h_{SR}|^2$, and $I_R = \sum_{i=1}^{N} P_{Ri}|g_{Ri}|^2$.

The relay has limited energy resources, and the energy is harvested on the basis of the time switching scheme
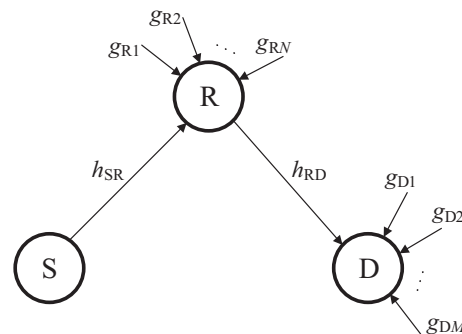

Fig. 1. System model.

from both the source and interference signals. The first part αT ($0 \le \alpha \le 1$) of each frame T is used for energy harvesting, and the total energy is $E_{\mathrm{H}} = \eta\big(P_{\mathrm{S}}|h_{\mathrm{SR}}|^2 + \sum_{i=1}^{N} P_{\mathrm{R}i}|g_{\mathrm{R}i}|^2\big)\alpha T$, where η is the energy conversion efficiency coefficient. The remaining time $(1-\alpha)T$ is split into two equal parts. The first part is dedicated to the transmission of the information signal to the relay, whereas the second part includes the transmission of the information signal from the relay to the destination.

As the electronic devices implemented in the energy harvester at the relay are nonlinear elements, we apply a nonlinear model for the energy harvester [21]. The harvested energy is linearly proportional to the input power for the values below the saturation threshold power P_{th}. A further increase in the input power does not lead to an additional increase in the harvested energy, as the saturation effect occurs. Therefore, the transmit power of the relay can be expressed as

$$P_{\mathrm{R}} = \frac{E_{\mathrm{H}}}{(1-\alpha)T/2} = \begin{cases} \frac{2\eta\alpha}{1-\alpha}(\gamma_{\mathrm{SR}} + I_{\mathrm{R}}), & \gamma_{\mathrm{SR}} + I_{\mathrm{R}} \le P_{\mathrm{th}}, \\ \frac{2\eta\alpha P_{\mathrm{th}}}{1-\alpha}, & \gamma_{\mathrm{SR}} + I_{\mathrm{R}} > P_{\mathrm{th}}. \end{cases}$$
(3)

We assume that the destination is corrupted by the total number of interference signals M, which are not used for energy harvesting and have only a degrading effect on signal detection. The signal at the destination is given by

$$y_{\mathrm{D}} = \sqrt{P_{\mathrm{R}}}h_{\mathrm{RD}}s_{\mathrm{R}} + \sum_{i=1}^{M} \sqrt{P_{\mathrm{D}i}}g_{\mathrm{D}i}s_{\mathrm{D}i},$$
(4)

where s_{R} is the signal transmitted from the relay, $s_{\mathrm{D}i}$ is ith interference signal with the power $P_{\mathrm{D}i}$ ($i = 1, \ldots, M$), and h_{RD} and $g_{\mathrm{D}i}$ are the channel fading gains of the second hop between R and D and from ith interference signal, respectively. At the destination, the SIR (in the interference-limited environment) is given as

$$\gamma_{\mathrm{D}} = \frac{P_{\mathrm{R}}|h_{\mathrm{RD}}|^2}{\sum_{i=1}^{M} P_{\mathrm{D}i}|g_{\mathrm{D}i}|^2} = P_{\mathrm{R}}\frac{\gamma_{\mathrm{RD}}}{I_{\mathrm{D}}},$$
(5)

where $\gamma_{\mathrm{RD}} = |h_{\mathrm{RD}}|^2$, and $I_{\mathrm{D}} = \sum_{i=1}^{M} P_{\mathrm{D}i}|g_{\mathrm{D}i}|^2$. On the basis of (3) and (5), the SIR at the destination can be rewritten as

$$\gamma_{\mathrm{D}} = \begin{cases} \frac{2\eta\alpha}{1-\alpha}\frac{\gamma_{\mathrm{RD}}}{I_{\mathrm{D}}}(\gamma_{\mathrm{SR}} + I_{\mathrm{R}}), & \gamma_{\mathrm{SR}} + I_{\mathrm{R}} \le P_{\mathrm{th}}, \\ \frac{2\eta\alpha}{1-\alpha}\frac{\gamma_{\mathrm{RD}}}{I_{\mathrm{D}}}P_{\mathrm{th}}, & \gamma_{\mathrm{SR}} + I_{\mathrm{R}} > P_{\mathrm{th}}. \end{cases}$$
(6)

In the considered system, the Nakagami-m distribution of fading is assumed, and the distribution of the random

variables (RVs) γ_{SR} and γ_{RD} can be described by the Gamma probability density function (PDF) [23]

$$f_\gamma(x) = \frac{1}{\Gamma(m)}\left(\frac{m}{\Omega}\right)^m x^{m-1}\exp\left(-\frac{mx}{\Omega}\right).$$
(7)

The fading parameters m and $\Omega = \mathrm{E}[x^2]$ are denoted as $(m_{\mathrm{SR}}, \Omega_{\mathrm{SR}})$ and $(m_{\mathrm{RD}}, \Omega_{\mathrm{RD}})$ for the S–R and R–D channels, respectively; $\mathrm{E}[\cdot]$ denotes the mathematical expectation, and $\Gamma(\cdot)$ is the Gamma function [24, (8.310.1)].

All interference links at both the relay and destination are subject to independent Nakagami-m fading. Therefore, the power of the sum of N identical interference signals at the relay, I_{R}, follows a Gamma distribution with the parameters m_{IR} and Ω_{IR} as

$$f_{\mathrm{IR}}(x) = \frac{1}{\Gamma(Nm_{\mathrm{IR}})}\left(\frac{m_{\mathrm{IR}}}{\Omega_{\mathrm{IR}}}\right)^{Nm_{\mathrm{IR}}} x^{Nm_{\mathrm{IR}}-1}\exp\left(-\frac{m_{\mathrm{IR}}x}{\Omega_{\mathrm{IR}}}\right).$$
(8)

The PDF of the total power of M interference signals at the destination I_{D} is described by the following expression:

$$f_{\mathrm{ID}}(x) = \frac{1}{\Gamma(Mm_{\mathrm{ID}})}\left(\frac{m_{\mathrm{ID}}}{\Omega_{\mathrm{ID}}}\right)^{Mm_{\mathrm{ID}}} x^{Mm_{\mathrm{ID}}-1}\exp\left(-\frac{m_{\mathrm{ID}}x}{\Omega_{\mathrm{ID}}}\right).$$
(9)

III. Outage Probability

In this section, we investigate the outage probability as an important system performance metric and provide a novel closed-form expression. The outage probability in the considered DF relaying system is defined as the probability that the received SIR at the relay or destination falls below predetermined threshold, γ_{th}, that is,

$$\begin{aligned} P_{\mathrm{OUT}}(\gamma_{\mathrm{th}}) &= F_{\mathrm{eq}}(\gamma_{\mathrm{th}}) \\ &= \Pr\{\gamma_{\mathrm{R}} \le \gamma_{\mathrm{th}}\} + \Pr\{\gamma_{\mathrm{D}} \le \gamma_{\mathrm{th}}, \gamma_{\mathrm{R}} > \gamma_{\mathrm{th}}\}, \end{aligned}$$
(10)

which can further be expressed as

$$\begin{aligned} P_{\mathrm{OUT}}(\gamma_{\mathrm{th}}) =\ & \Pr\{v \le \gamma_{\mathrm{th}}\} \\ & + \Pr\left\{u \le \frac{\gamma_{\mathrm{th}}}{w}, w > \frac{\gamma_{\mathrm{th}}}{P_{\mathrm{th}}}, v > \gamma_{\mathrm{th}}\right\} \\ & + \Pr\left\{w \le \frac{\gamma_{\mathrm{th}}}{P_{\mathrm{th}}}, v > \gamma_{\mathrm{th}}\right\} \\ =\ & \Im_1 + \Im_2 + \Im_3, \end{aligned}$$
(11)

where $v = \gamma_{\mathrm{SR}}/I_{\mathrm{R}}$, $u = \gamma_{\mathrm{SR}} + I_{\mathrm{R}}$, and $w = 2\eta\alpha\gamma_{\mathrm{RD}}/((1-\alpha)I_{\mathrm{D}})$.

By using the changes in the RVs and the appropriate mathematical manipulations, as described in Appendix I, the expression $\Im_1$ in (11) is defined and solved as

$$\Im_1 = \Pr\{v \le \gamma_{\text{th}}\} = \Theta_1 \lambda_1{}^{m_{\text{SR}}} \gamma_{\text{th}}{}^{m_{\text{SR}}}$$
$$\times {}_2F_1(m_{\text{SR}}, m_{\text{SR}} + Nm_{\text{IR}}; m_{\text{SR}} + 1; -\lambda_1 \gamma_{\text{th}}), \quad (12)$$

where $\lambda_1 = m_{\text{SR}}\Omega_{\text{IR}}/m_{\text{IR}}\Omega_{\text{SR}}$, $\Theta_1 = (1/m_{\text{SR}})[(\Gamma(m_{\text{SR}} + Nm_{\text{IR}}))/(\Gamma(m_{\text{SR}})\Gamma(Nm_{\text{IR}}))]$, and ${}_2F_1(a, b; c; z)$ denotes the Gaussian hypergeometric function defined in [25, (07.23.02.0001.01)].

The second expression $\Im_2$ in (11) is defined as

$$\Im_2 = \Pr\left\{u \le \frac{\gamma_{\text{th}}}{w}, w > \frac{\gamma_{\text{th}}}{P_{\text{th}}}, v > \gamma_{\text{th}}\right\}$$
$$= \int_{\frac{\gamma_{\text{th}}}{P_{\text{th}}}}^{\infty} \left(\int_{\gamma_{\text{th}}}^{\infty} \int_0^{\frac{\gamma_{\text{th}}}{w}} f_{u,v}(u, v) \mathrm{d}u \mathrm{d}v \right) f_w(w) \mathrm{d}w . \quad (13)$$

The joint PDF of the RVs u and $v, f_{u,v}(u, v)$, and the PDF of the RV w are derived in Appendix I. The triple integral $\Im_2$ defined in the previous equation is solved by following the derivation given in the Appendices and can be written as

$$\Im_2 = \sum_{k=0}^{m_{\text{SR}}-1} \Xi(k)\, (1 - \lambda_1)^{-Nm_{\text{IR}}-k} \left[\Im_{21} - \Im_{22} \right.$$
$$- \sum_{p=0}^{Nm_{\text{IR}}+k-1} \frac{\lambda_1{}^{m_{\text{SR}}}}{p!} \times \left(\frac{1-\lambda_1}{1+\gamma_{\text{th}}\lambda_1}\right)^p \left(\frac{\gamma_{\text{th}}+1}{1+\gamma_{\text{th}}\lambda_1}\right)^{m_{\text{SR}}-k}$$
$$\left. \times (\Im_{23} - \Im_{24}) \right], \quad (14)$$

where $\Xi(k) = \frac{\Gamma(Nm_{\text{IR}}+k)}{\Gamma(m_{\text{SR}})\Gamma(Nm_{\text{IR}})} \binom{m_{\text{SR}}-1}{k}(-1)^k$, and the expressions $\Im_{2k}, k = 1, 2, 3, 4$ are defined and solved in the Appendices and presented in their exact closed forms in the following. The first expression $\Im_{21}$ is given by

$$\Im_{21} = \lambda_1{}^k \Gamma(m_{\text{SR}} - k) \frac{m_{\text{RD}}}{Mm_{\text{ID}}} \Theta_2 \left(\frac{\lambda_5}{\lambda_2}\right)^{Mm_{\text{ID}}}$$
$$\times {}_2F_1\left(m_{\text{RD}} + Mm_{\text{ID}}, Mm_{\text{ID}}; Mm_{\text{ID}} + 1; -\frac{\lambda_5}{\lambda_2}\right). \quad (15)$$

The second expression $\Im_{22}$ in (14) can be presented in an exact closed form as

$$\Im_{22} = \lambda_1{}^k m_{\text{RD}} \Theta_2 \lambda_2{}^{m_{\text{RD}}} \Gamma(m_{\text{SR}} - k) \exp(\lambda_2 \lambda_3)$$
$$\times \sum_{r=0}^{m_{\text{SR}}-k-1} \sum_{s=0}^{Mm_{\text{ID}}-1+r} \binom{Mm_{\text{ID}}-1+r}{s} \frac{\lambda_3{}^r}{r!}(-\lambda_2)^{Mm_{\text{ID}}-1+r-s}$$
$$\times \left(\lambda_2{}^{1+s-m_{\text{RD}}-Mm_{\text{ID}}} E_{m_{\text{RD}}+Mm_{\text{ID}}-s}(\lambda_2\lambda_3) \right.$$
$$\left. -(\lambda_2+\lambda_5)^{1+s-m_{\text{RD}}-Mm_{\text{ID}}} E_{m_{\text{RD}}+Mm_{\text{ID}}-s}(\lambda_3(\lambda_2+\lambda_5)) \right), \quad (16)$$

and the third expression $\Im_{23}$ can be written in the following form:

$$\Im_{23} = \Gamma(m_{\text{SR}} - k + p) \frac{m_{\text{RD}}}{Mm_{\text{ID}}} \Theta_2 \left(\frac{\lambda_5}{\lambda_2}\right)^{Mm_{\text{ID}}}$$
$$\times {}_2F_1\left(m_{\text{RD}} + Mm_{\text{ID}}, Mm_{\text{ID}}; Mm_{\text{ID}} + 1; -\frac{\lambda_5}{\lambda_2}\right). \quad (17)$$

The closed-form solution for $\Im_{24}$ is given by

$$\Im_{24} = m_{\text{RD}} \Theta_2 \lambda_2{}^{m_{\text{RD}}} \Gamma(m_{\text{SR}} - k + p) \exp(\lambda_2 \lambda_4)$$
$$\times \sum_{l=0}^{m_{\text{SR}}-k+p-1} \sum_{q=0}^{Mm_{\text{ID}}-1+l} \binom{Mm_{\text{ID}}-1+l}{q}$$
$$\times (-\lambda_2)^{Mm_{\text{ID}}-1+l-q} \frac{\lambda_4{}^l}{l!}$$
$$\times \left(\lambda_2{}^{1+q-m_{\text{RD}}-Mm_{\text{ID}}} E_{m_{\text{RD}}+Mm_{\text{ID}}-q}(\lambda_2\lambda_4) \right.$$
$$\left. -(\lambda_2+\lambda_5)^{1+q-m_{\text{RD}}-Mm_{\text{ID}}} E_{m_{\text{RD}}+Mm_{\text{ID}}-q}(\lambda_4(\lambda_2+\lambda_5)) \right), \quad (18)$$

where $E_v(x)$ is the exponential integral [25, (06.34.02.0001.01)], and the parameters are defined as $\Theta_2 = \frac{\Gamma(m_{\text{RD}}+Mm_{\text{ID}})}{m_{\text{RD}}\Gamma(m_{\text{RD}})\Gamma(Mm_{\text{ID}})}$, $c = \frac{2\eta\alpha}{(1-\alpha)}$, $\lambda_2 = \frac{m_{\text{RD}}\Omega_{\text{ID}}}{m_{\text{ID}}\Omega_{\text{RD}}c}$, $\lambda_3 = \frac{m_{\text{SR}}}{\Omega_{\text{SR}}}\gamma_{\text{th}}$, $\lambda_5 = \frac{P_{\text{th}}}{\gamma_{\text{th}}}$, and $\lambda_4 = \frac{\gamma_{\text{th}}}{1+\gamma_{\text{th}}}\frac{m_{\text{IR}}}{\Omega_{\text{IR}}}\left(1 + \gamma_{\text{th}}\frac{m_{\text{SR}}\Omega_{\text{IR}}}{m_{\text{IR}}\Omega_{\text{SR}}}\right)$.

Finally, the expression $\Im_3$ defined in (11) is solved by applying the mathematical manipulations presented in Appendix I, and the closed-form solution is given by the following formula:

$$\Im_3 = \Pr\left\{w \le \frac{\gamma_{\text{th}}}{P_{\text{th}}}, v > \gamma_{\text{th}}\right\} = \Pr\left\{w \le \frac{\gamma_{\text{th}}}{P_{\text{th}}}\right\} \Pr\{v > \gamma_{\text{th}}\}$$
$$= \Theta_2 \left(\frac{\lambda_2}{\lambda_5}\right)^{m_{\text{RD}}} {}_2F_1\left(m_{\text{RD}}, m_{\text{RD}} + Mm_{\text{ID}}; m_{\text{RD}} + 1; -\frac{\lambda_2}{\lambda_5}\right)$$
$$\times \left(1 - \Theta_1 \lambda_1{}^{m_{\text{SR}}} \gamma_{\text{th}}{}^{m_{\text{SR}}} {}_2F_1(m_{\text{SR}}, m_{\text{SR}} + Nm_{\text{IR}}; m_{\text{SR}} + 1; -\lambda_1\gamma_{\text{th}})\right). \quad (19)$$

By substituting the derived closed form-expressions in (12) and (14) to (19) into (11), we obtain the final closed-form expression for the outage probability.

1. Special Cases

Remark 1. When the power of the signal is dominant compared to the power of the interference at the relay, the parameters λ_1 and λ_3 asymptotically approach a value of zero. Consequently, the expressions $\Im_1 \to 0$ and $\Im_2 \to 0$, and the asymptotic expression for the outage probability is given by

$$P_{\text{out}} \approx \Theta_2 \left(\frac{\lambda_2}{\lambda_5}\right)^{m_{\text{RD}}} {}_2\text{F}_1\left(m_{\text{RD}}, m_{\text{RD}} + Mm_{\text{ID}}; m_{\text{RD}} + 1; -\frac{\lambda_2}{\lambda_5}\right).$$

(20)

Remark 2. When the SIR at the destination node is large, the parameter $\lambda_2 \to 0$, and the asymptotic expression for the outage probability is given by the expression $\Im_1$, that is,

$$P_{\text{out}} \approx \Theta_1 {\lambda_1}^{m_{\text{SR}}} \gamma_{\text{th}}^{m_{\text{SR}}}$$
$$\times {}_2\text{F}_1\left(m_{\text{SR}}, m_{\text{SR}} + Nm_{\text{IR}}; m_{\text{SR}} + 1; -\lambda_1 \gamma_{\text{th}}\right).$$

(21)

Remark 3. When $P_{\text{th}} \to \infty$, the parameter $\lambda_5 \to \infty$, and the outage probability expression in (11) that is valid for the interference-limited scenario and the general case of the nonlinear harvesting model is simplified to the expression valid for the linear model. Since the expression $\Im_3 \to 0$ when $\lambda_5 \to \infty$ according to [25, (07.23.06.0001.02)] and the expression $\Im_1$ in (12) does not depend on P_{th}, the outage probability is given by

$$P_{\text{out}}^{P_{\text{th}} \to \infty} = \Im_1 + \Im_2^{P_{\text{th}} \to \infty}.$$

(22)

After applying $\lambda_5 \to \infty$ and the identity in [25, (07.23.06.0023.01)] to (15) and (17), we derive $\Im_{21}^{P_{\text{th}} \to \infty}$ and $\Im_{23}^{P_{\text{th}} \to \infty}$, respectively, as

$$\Im_{21}^{P_{\text{th}} \to \infty} = {\lambda_1}^k \Gamma(m_{\text{SR}} - k),$$

(23)

$$\Im_{23}^{P_{\text{th}} \to \infty} = \Gamma(m_{\text{SR}} - k + p).$$

(24)

By utilizing the identity in [25, (06.34.03.0014.01)] in (16) and (18), we obtain the following results for $\Im_{22}^{P_{\text{th}} \to \infty}$ and $\Im_{24}^{P_{\text{th}} \to \infty}$, respectively:

$$\Im_{22}^{P_{\text{th}} \to \infty} = {\lambda_1}^k m_{\text{RD}} \Theta_2 \Gamma(m_{\text{SR}} - k) \exp(\lambda_2 \lambda_3)$$
$$\times \sum_{r=0}^{m_{\text{SR}}-k-1} \sum_{s=0}^{Mm_{\text{ID}}-1+r} \binom{Mm_{\text{ID}} - 1 + r}{s} \frac{(\lambda_2 \lambda_3)^r}{r!}$$
$$\times (-1)^{Mm_{\text{ID}}-1+r-s} E_{m_{\text{RD}}+Mm_{\text{ID}}-s}(\lambda_2 \lambda_3),$$

(25)

$$\Im_{24}^{P_{\text{th}} \to \infty} = m_{\text{RD}} \Theta_2 \Gamma(m_{\text{SR}} - k + p) \exp(\lambda_2 \lambda_4)$$
$$\times \sum_{l=0}^{m_{\text{SR}}-k+p-1} \sum_{q=0}^{Mm_{\text{ID}}-1+l} \binom{Mm_{\text{ID}} - 1 + l}{q} \frac{(\lambda_2 \lambda_4)^l}{l!}$$
$$\times (-1)^{Mm_{\text{ID}}-1+l-q} E_{m_{\text{RD}}+Mm_{\text{ID}}-q}(\lambda_2 \lambda_4).$$

(26)

By substituting the expressions in (12), (14), and (23) to (26) into (22), we derive the closed-form outage probability expression for the case when a simple linear energy-harvesting model at the relay is applied.

IV. Numerical Results

The outage performance is examined for various system and fading parameters in this section. The accuracy of the derived analytical expressions and corresponding asymptotic approximations are corroborated by the independent simulation method. Fading envelope waveform sequences with $L = 10^7$ samples are generated for both links from the source to the relay and from the relay to the destination as well as for all links from the interference sources to the relay and destination. The outage performance is evaluated by averaging over successive channel realizations. The numerical results for the outage probability are provided using the closed-form expression, which is obtained by substituting the expressions in (12) and (14) to (18) into (11).

In Fig. 2, the dependence of the outage probability on the average signal power in the S–R link Ω_{SR} is presented for different values of the interference signal power Ω_{IR} and saturation threshold power P_{th}. Although the derived analytical expressions are valid in general, for the numerical analysis of the outage probability, we set the parameters to $\gamma_{\text{th}} = -5$ dB, $m_{\text{SR}} = 1$, $m_{\text{RD}} = m_{\text{ID}} = m_{\text{IR}} = 2$, and $\Omega_{\text{ID}} = 0$ dB. From the results shown, it can be observed that the outage probability decreases with the increase in the parameter Ω_{SR}. Furthermore, the increase in P_{th} leads to better system performance. The increase in the interference power has a negative influence on the system performance, as was previously noted in [17] for the linear harvesting model. From the results presented in Fig. 2 for the nonlinear energy harvester model, it is noted that the influence of the interference is more dominant for larger values of the saturation threshold power. Moreover, we can see that for very low values of the signal power Ω_{SR}, the
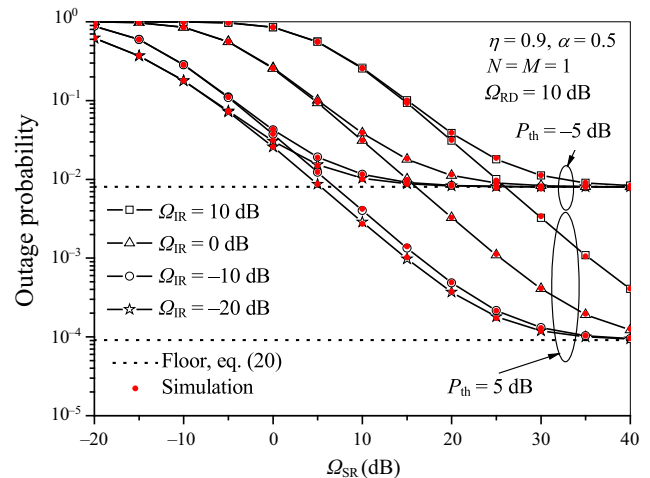

Fig. 2. Outage probability vs. average signal power for S–R link.

impact of P_{th} on the outage probability diminishes. This result can be explained by the fact that for small Ω_{SR}, the total input power is lower than the threshold value P_{th}. For large values of Ω_{SR}, an outage floor occurs, and the value of the floor is determined by the derived asymptotic expression in (20). Moreover, the value of the outage floor decreases for increasing values of P_{th}.

In Fig. 3, the outage probability is presented as a function of the energy-harvesting ratio α for different numbers of independent interference signals at the destination M and various values of the threshold power P_{th}. For all analyzed cases, the outage probability decreases as the values of the energy-harvesting ratio α and harvesting threshold power P_{th} increase. Moreover, the outage probability becomes worse for a larger number of interference signals M. However, for high values of α, the influence of the number of interference signals and threshold power diminishes. The outage probability is then determined by the approximate expression in (21), that is, by the parameter values of the first hop. In this case, the number of interference signals, that is, the interference power at the destination, and P_{th} do not have a significant influence on the outage probability.

Figure 4 presents the outage probability as a function of the threshold power P_{th} for different values of the parameter α and the average signal power for the S–R link Ω_{SR}. The outage performance is improved as the average power of the first link increases. Owing to the nonlinearity of the energy-harvesting model, the outage probability significantly decreases as the threshold power increases. However, at high values of P_{th}, an outage probability floor exists, and the system acts as one with linear energy harvesting. This outage probability floor is determined by substituting the closed-form expressions in (12), (14), and

(23) to (26) into (22). The minimum value of P_{th} where the outage floor occurs is increased for higher values of the average power Ω_{SR} and smaller values of α. The outage probability also decreases with the increase in the parameter α, but as shown in Fig. 3, this difference is not significant for larger parameter values (therefore, the curves for $\alpha = 0.5$ and $\alpha = 0.9$ overlap in the floor region).

In Figs. 5 and 6, the achievable throughput T_{out} of the interference-limited nonlinear energy-harvesting DF system is analyzed as an important outage performance metric [17], [23]. The achievable throughput is given by

$$T_{out} = (1 - \alpha)C_{out}, \tag{27}$$

where C_{out} is outage capacity of the system defined as

$$C_{out} = 0.5 \times \left(1 - P_{out}(\gamma_{th})\right)\log_2(1 + \gamma_{th}). \tag{28}$$

The outage capacity is the maximum data rate that can be achieved in the channel with the outage probability $P_{out} = \Pr(\gamma < \gamma_{th})$ that occurs when the channel is in deep fading. The factor 0.5 is included in (28) since the total communication time is divided into two equal parts dedicated to transmission from the source to the relay and from the relay to the destination. Finally, as the information is transferred only during the time $(1 - \alpha)T$ of the frame T, the achievable throughput is given by (27).

The dependence of the throughput T_{out} on α is presented in Fig. 5 for various numbers of independent interference signals at the relay and destination. The outage threshold is set to $\gamma_{th} = 5$ dB. It is noted that for the optimal value of α, a maximum value exists for T_{out}, which is dependent on the number of interference signals at the relay and destination, that is, the total power of the interference signals. The optimal value of α is lower when the number of interference
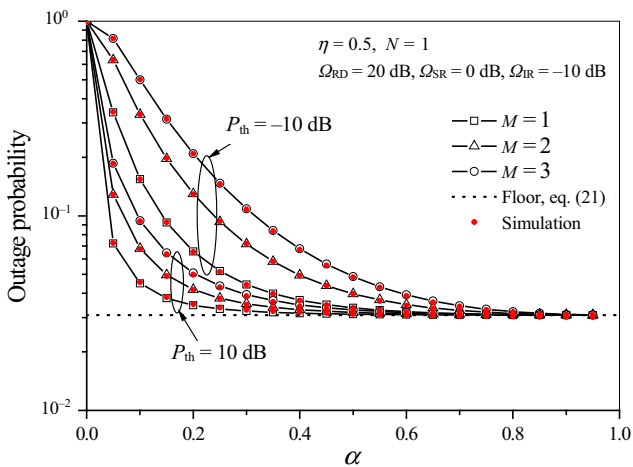
Fig. 3. Outage probability vs. energy-harvesting ratio α for various numbers of interference signals at D.
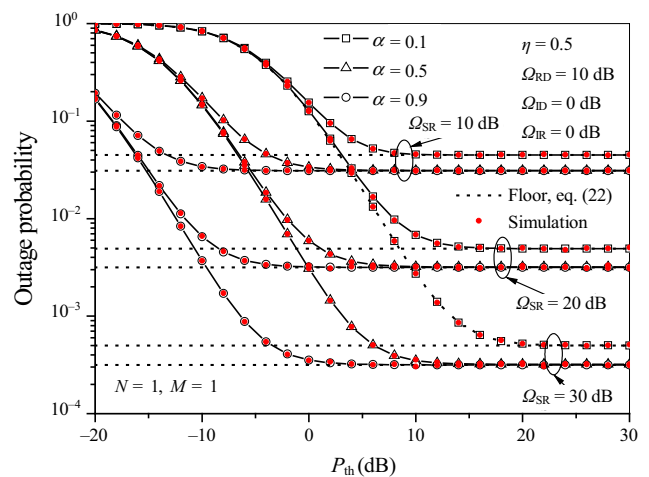
Fig. 4. Outage probability vs. saturation threshold power P_{th}.

signals at the relay N is greater. In other words, the increased power of the interference signals at the relay results in a lower optimal value of α, meaning that the optimal time for energy harvesting is shorter. At the same time, a degradation in the system performance (T_{out}) occurs. On the other hand, when the number of interference signals at the destination M is increased, a deterioration in the system performance also occurs, but a longer harvesting time is needed to achieve the maximum T_{out}. The interference signals at the destination are not involved in energy harvesting but only lead to the performance degradation.

Figure 6 shows the throughput T_{out} as a function of the energy-harvesting ratio α for different values of the Nakagami-m fading parameters and saturation threshold power P_{th}. Higher values of the fading parameters lead to an increased achievable throughput for all values of α. Furthermore, for all analyzed parameter values, a maximum
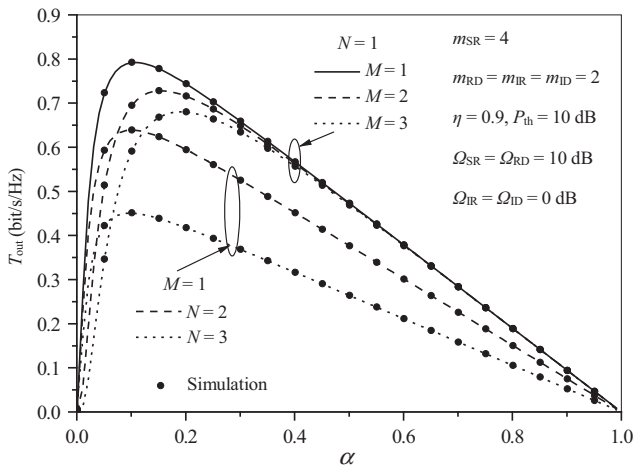

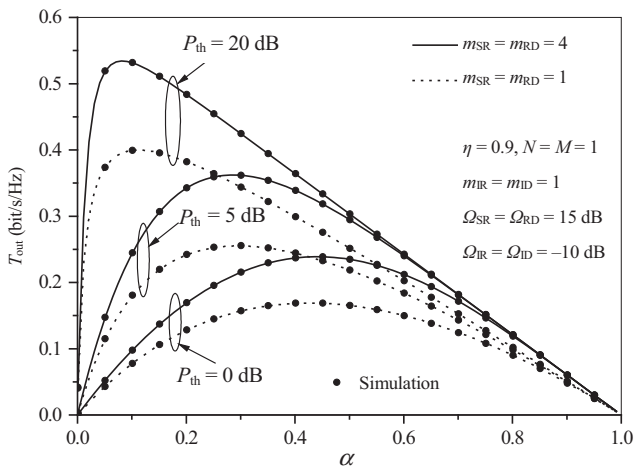Fig. 5. Throughput T_{out} vs. α for various numbers of interference signals.

Fig. 6. Throughput T_{out} vs. energy-harvesting ratio α for various values of P_{th} and fading conditions.
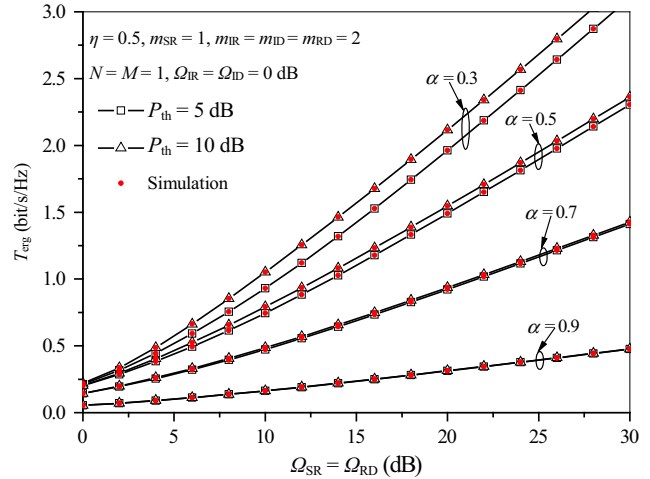

Fig. 7. Throughput T_{erg} vs. average signal power $\Omega_{SR} = \Omega_{RD}$ for various values of P_{th} and energy-harvesting ratio α.

value for the throughput and the corresponding optimal ratio α exist. For a greater threshold power P_{th}, the optimal value of α is lower, and the maximum T_{out} is increased. This effect can be explained by the fact that when the values of P_{th} are small owing to the nonlinearity and power limitation, a longer time is needed to harvest the optimal energy.

The ergodic capacity is also an important metric for the spectral efficiency applicable to systems with no delay limitations. It represents the maximum long-term rate that can be achieved with an arbitrarily small probability of error and can be calculated as [17, (21)]

$$C_{erg} = \frac{1}{2\ln 2} \int_0^\infty \frac{1 - F_{eq}(\gamma)}{1 + \gamma} d\gamma, \qquad (29)$$

and the achievable throughput can be obtained as

$$T_{erg} = (1 - \alpha)C_{erg}. \qquad (30)$$

By utilizing (29) and (30), we have obtained numerical and simulation results for T_{erg} that are presented in Fig. 7 for various values of P_{th} and the energy-harvesting ratio α. It is noted that lower values of the energy-harvesting ratio α result in greater values of the achievable throughput, as more time is spent for information encoding and transmission in this case. On the other hand, greater values of α mean that more time is spent on energy harvesting, which results in worse system performance. In addition, as the energy-harvesting ratio increases, the impact of the threshold power on the system performance diminishes.

V. Conclusion

This paper has analyzed a DF relay system based on a realistic nonlinear model, in which a relay harvests

energy. Besides the desired signal from the source, the relay is powered by interference signals using the time switching scheme. Closed-form expressions for the outage probability and achievable throughput have been derived for the interference-limited case and Nakagami-m fading environment. Furthermore, an analysis is provided for high average SNR values, and an outage expression for a simpler linear harvesting model is also derived. Simulation results are presented, and the accuracy of the derived analytical results is confirmed.

It has been concluded that an outage probability floor exists in the range of large values of the average power of the S–R link. This outage probability floor is highly dependent on the nonlinearity of the electronic devices in relay energy harvester (that is, the value of the saturation threshold power). This means that a further increase in the desired signal power will not improve the system performance. Furthermore, when the average power of the R–D link and the energy-harvesting ratio are high, the effects of the number of interference signals at the destination and the threshold power on the outage performance are diminished. It can be observed that in the case of a large threshold power, the considered system acts similar to the linear one. On the basis of the results for the achievable throughput, it has been noted that an optimal value exists for the energy-harvesting ratio, which maximizes the system throughput. This optimal value is lower when the number of interference signals and their power at the relay are increased as well as when the number of interference signals and their power at the destination are decreased. In addition, the optimal value of the energy-harvesting ratio is greater when the saturation threshold power is lower.

Acknowledgements

Appendix I

In order to determine the expression $\Im_1$, we need the cumulative density function (CDF) of the ratio $v = \gamma_{SR}/I_R$, which can be calculated using [26, (7.23)]: $F_v(\gamma_{th}) = \Pr\{v \le \gamma_{th}\} = \int_0^{\gamma_{th}} \int_0^\infty x f_{\gamma_{SR}}(ux) f_{IR}(x) dx du$.

After applying [24, (3.351.3)] and [24, (3.194.1)], the expression $\Im_1$ is solved and given in (12).

In order to obtain the integrals $\Im_2$ and $\Im_3$, a statistic for the RV $w = 2\eta\alpha\gamma_{RD}/((1-\alpha)I_D)$ is required. Using

$f_w(w) = \int_0^\infty x f_{\gamma_{RD}}(ux) f_{ID}(x) dx$, we obtain the PDF of w in the following form:

$$f_w(w) = \frac{\Gamma(m_{RD} + Mm_{ID})}{\Gamma(m_{RD})\Gamma(Mm_{ID})} \left(\frac{m_{RD}\Omega_{ID}}{cm_{ID}\Omega_{RD}}\right)^{m_{RD}}$$
$$\times \frac{w^{m_{RD}-1}}{\left(\frac{m_{RD}\Omega_{ID}w}{m_{ID}\Omega_{RD}c} + 1\right)^{m_{RD}+Mm_{ID}}}. \quad (A1)$$

In a similar manner, we can find the CDF of w as

$$\Pr\left\{w \le \frac{\gamma_{th}}{P_{th}}\right\} = A_2\left(\frac{\lambda_2}{\lambda_5}\right)^{m_{RD}}$$
$$\times \; _2F_1\left(m_{RD}, \; m_{RD} + Mm_{ID}, \; m_{RD} + 1, \; -\frac{\lambda_2}{\lambda_5}\right). \quad (A2)$$

To solve the integral $\Im_2$, the joint PDF for $u = (\gamma_{SR} + I_R)$ and $v = \gamma_{SR}/I_R$ is needed. With the help of $f_{u,v}(u,v) = |J| f_{\gamma_{SR}}(uv/(v+1)) f_{IR}(u/(v+1))$ [26, (7-37)], where $|J| = u/(v+1)^2$ is the Jacobian determinant, and by replacing the appropriate PDFs, the joint PDF is found to be

$$f_{u,v}(u,v) = \frac{u^{m_{SR}-1+Nm_{IR}} v^{m_{SR}-1}}{\Gamma(m_{SR})\Gamma(Nm_{IR})} \left(\frac{m_{SR}}{\Omega_{SR}}\right)^{m_{SR}} \left(\frac{m_{IR}}{\Omega_{IR}}\right)^{Nm_{IR}}$$
$$\times \left(\frac{1}{v+1}\right)^{Nm_{IR}+m_{SR}} \exp\left(-\frac{m_{SR}}{\Omega_{SR}}\frac{uv}{v+1}\right) \exp\left(-\frac{m_{IR}}{\Omega_{IR}}\frac{u}{v+1}\right). \quad (A3)$$

Appendix II

The first step in the process of solving the integral $\Im_2$ is to find $\int_{\gamma_{th}}^\infty f_{u,v}(u,v) dv$. After substituting $t = (v+1)^{-1}$ into (A3), applying the binomial theorem, and using [24, (3.351.2)], the integral is obtained as

$$\int_{\gamma_{th}}^\infty f_{u,v}(u,v) dv = \sum_{k=0}^{m_{SR}-1} \binom{m_{SR}-1}{k} (-1)^k \left(\frac{m_{SR}}{\Omega_{SR}}\right)^{m_{SR}} \left(\frac{m_{IR}}{\Omega_{IR}}\right)^{-k}$$
$$\times \left(1 - \frac{m_{SR}\Omega_{IR}}{m_{IR}\Omega_{SR}}\right)^{-Nm_{IR}-k} \frac{\Gamma(Nm_{IR}+k)}{\Gamma(m_{SR})\Gamma(Nm_{IR})}$$
$$\times \left(u^{m_{SR}-1-k} \exp\left(-\frac{m_{SR}u}{\Omega_{SR}}\right) - e^{-\frac{1}{\gamma_{th}+1}\left(\frac{m_{IR}}{\Omega_{IR}} - \frac{m_{SR}}{\Omega_{SR}}\right)u - \frac{m_{SR}u}{\Omega_{SR}}}$$
$$\times \sum_{p=0}^{Nm_{IR}+k-1} \frac{1}{p!} \left(\frac{1}{\gamma_{th}+1}\left(\frac{m_{IR}}{\Omega_{IR}} - \frac{m_{SR}}{\Omega_{SR}}\right)\right)^p u^{m_{SR}-1-k+p}\right). \quad (A4)$$

Further, the integration of (A4) with respect to v is performed on the basis of [24, (3.351.1)] as

$$\int_0^{\gamma_{\text{th}}/w}\int_{\gamma_{\text{th}}}^{\infty}f_{u,v}(u,v)\mathrm{d}v\mathrm{d}u=\sum_{k=0}^{m_{\text{SR}}-1}\frac{\Gamma(Nm_{\text{IR}}+k)}{\Gamma(m_{\text{SR}})\Gamma(Nm_{\text{IR}})}$$

$$\times\binom{m_{\text{SR}}-1}{k}(-1)^k\left(1-\frac{m_{\text{SR}}\Omega_{\text{IR}}}{m_{\text{IR}}\Omega_{\text{SR}}}\right)^{-Nm_{\text{IR}}-k}$$

$$\times\left(\left(\frac{m_{\text{SR}}\Omega_{\text{IR}}}{m_{\text{IR}}\Omega_{\text{SR}}}\right)^k\cdot\left(\Gamma(m_{\text{SR}}-k)-\Gamma\left(m_{\text{SR}}-k,\frac{m_{\text{SR}}}{\Omega_{\text{SR}}}\frac{\gamma_{\text{th}}}{w}\right)\right)\right.$$

$$-\sum_{p=0}^{Nm_{\text{IR}}+k-1}\frac{1}{p!}\left(1-\frac{m_{\text{SR}}\Omega_{\text{IR}}}{m_{\text{IR}}\Omega_{\text{SR}}}\right)^p\left(\frac{1}{\gamma_{\text{th}}+1}\right)^{-m_{\text{SR}}+k}\left(\frac{m_{\text{SR}}\Omega_{\text{IR}}}{m_{\text{IR}}\Omega_{\text{SR}}}\right)^{m_{\text{SR}}}$$

$$\times\left(1+\gamma_{\text{th}}\frac{m_{\text{SR}}\Omega_{\text{IR}}}{m_{\text{IR}}\Omega_{\text{SR}}}\right)^{-m_{\text{SR}}+k-p}\left(\Gamma(m_{\text{SR}}-k+p).\right.$$

$$\left.\left.-\Gamma\left(m_{\text{SR}}-k+p,\frac{1}{\gamma_{\text{th}}+1}\frac{m_{\text{IR}}}{\Omega_{\text{IR}}}\left(1+\gamma_{\text{th}}\frac{m_{\text{SR}}\Omega_{\text{IR}}}{m_{\text{IR}}\Omega_{\text{SR}}}\right)\frac{\gamma_{\text{th}}}{w}\right)\right)\right).\tag{A5}$$

In (A5), $\Gamma(\cdot,\cdot)$ is the incomplete Gamma function [24, (8.350.2)].

After substituting (A5) into (13) and using the corresponding replacement of parameters, the integral $\Im_2$ is rewritten as (14), where

$$\Im_{21}=\int_{\frac{\gamma_{\text{th}}}{P_{\text{th}}}}^{\infty}\lambda_1^k\Gamma(m_{\text{SR}}-k)m_{\text{RD}}\Theta_2\lambda_2^{m_{\text{RD}}}$$
$$\times\frac{w^{m_{\text{RD}}-1}}{(\lambda_2w+1)^{m_{\text{RD}}+Mm_{\text{ID}}}}\mathrm{d}w,\tag{A6}$$

$$\Im_{22}=\int_{\frac{\gamma_{\text{th}}}{P_{\text{th}}}}^{\infty}\lambda_1^k\Gamma\left(m_{\text{SR}}-k,\frac{m_{\text{SR}}}{\Omega_{\text{SR}}}\frac{\gamma_{\text{th}}}{w}\right)m_{\text{RD}}\Theta_2\lambda_2^{m_{\text{RD}}}$$
$$\times\frac{w^{m_{\text{RD}}-1}}{(\lambda_2w+1)^{m_{\text{RD}}+Mm_{\text{ID}}}}\mathrm{d}w,\tag{A7}$$

$$\Im_{23}=\int_{\frac{\gamma_{\text{th}}}{P_{\text{th}}}}^{\infty}\Gamma(m_{\text{SR}}-k+p)m_{\text{RD}}\Theta_2\lambda_2^{m_{\text{RD}}}$$
$$\times\frac{w^{m_{\text{RD}}-1}}{(\lambda_2w+1)^{m_{\text{RD}}+Mm_{\text{ID}}}}\mathrm{d}w,\tag{A8}$$

$$\Im_{24}=\int_{\frac{\gamma_{\text{th}}}{P_{\text{th}}}}^{\infty}\Gamma\left(m_{\text{SR}}-k+p,\frac{1}{\gamma_{\text{th}}+1}\frac{m_{\text{IR}}}{\Omega_{\text{IR}}}(1+\gamma_{\text{th}}\lambda_1)\frac{\gamma_{\text{th}}}{w}\right)$$
$$\times m_{\text{RD}}\Theta_2\lambda_2^{m_{\text{RD}}}\frac{w^{m_{\text{RD}}-1}}{(\lambda_2w+1)^{m_{\text{RD}}+Mm_{\text{ID}}}}\mathrm{d}w.\tag{A9}$$

The integrals $\Im_{21}$ and $\Im_{23}$ are solved by using [24, (3.194.2)], and the corresponding final closed-form

solutions are given in (15) and (17), respectively. To solve the integrals $\Im_{22}$ and $\Im_{24}$, the series representation of the Gamma function is performed on the basis of [24, (8.352.2)]. After applying the corresponding replacements $t=1/w$ and $x=a_2+t$ and by utilizing [24, (06.34.07.0001.01)], the final closed-form solutions of integrals $\Im_{22}$ and $\Im_{24}$ are derived and presented in (16) and (18), respectively.

References

[1] M. Dohler and Y. Li, *Cooperative Communications: Hardware, Channel and PHY*, Chichester, UK: John Wiley & Sons, 2010.

[2] M.-L. Ku et al., "Advances in Energy Harvesting Communications: Past, Present, and Future Challenges," *IEEE Commun. Surv. Tuts.*, vol. 18, no. 2, 2016, pp. 1384–1412.

[3] S. Ulukus et al., "Energy Harvesting Wireless Communications: A Review of Recent Advances," *IEEE J. Sel. Areas Commun.*, vol. 33, no. 3, Jan. 2015, pp. 360–381.

[4] S. Kosunalp, "MAC Protocols for Energy Harvesting Wireless Sensor Networks: Survey," *ETRI J.*, vol. 37, no. 4, Aug. 2015, pp. 804–812.

[5] C. Huang, R. Zhang, and S. Cui, "Throughput Maximization for the Gaussian Relay Channel with Energy Harvesting Constraints," *IEEE J. Sel. Areas Commun.*, vol. 31, no. 8, Aug. 2013, pp. 1469–1479.

[6] A.A. Nasir et al., "Relaying Protocols for Wireless Energy Harvesting and Information Processing," *IEEE Trans. Wireless Commun.*, vol. 12, no. 7, July 2013, pp. 3622–3636.

[7] L. Tang et al., "Wireless Information and Energy Transfer in Fading Relay Channels," *IEEE J. Sel. Areas Commun.*, vol. 34, no. 12, Sept. 2016, pp. 3632–3645.

[8] C. Zhong, S. Jin, and K.-K. Wong, "Dual-hop Systems with Noisy Relay and Interference-Limited Destination," *IEEE Trans. Commun.*, vol. 58, no. 3, Mar. 2010, pp. 764–768.

[9] D.B. da Costa, H. Ding, and J. Ge, "Interference-Limited Relaying Transmissions in Dual-Hop Cooperative Networks over Nakagami-*m* Fading," *IEEE Commun. Lett.*, vol. 15, no. 5, May 2011, pp. 503–505.

[10] S. Ikki and S. Aissa, "Multi-hop Wireless Relaying Systems in the Presence of Co-channel Interferences: Performance Analysis and Design Optimization," *IEEE Trans. Veh. Tech.*, vol. 61, no. 2, Feb. 2012, pp. 566–573.

[11] N. Zhao et al., "Exploiting Interference for Energy Harvesting: A Survey, Research Issues and Challenges," *IEEE Access*, vol. 5, May 2017, pp. 10403–10421.

[12] L. Liu, R. Zhang, and K.-C. Chua, "Wireless Information Transfer with Opportunistic Energy Harvesting," *IEEE Trans. Wireless Commun.*, vol. 12, no. 1, Jan. 2013, pp. 288–300.

[13] T.X. Doan et al., "Energy Harvesting-Based D2D Communications in the Presence of Interference and Ambient RF Sources," *IEEE Access*, vol. 5, Mar. 2017, pp. 5224–5234.

[14] Z. Xie, Y. Chen, and Y. Gao, "Joint Iterative Interference Alignment and Energy Harvesting for Multi-user Networks," *IEEE Wireless Commun. Lett.*, vol. 4, no. 6, Dec. 2015, pp. 597–600.

[15] R. Gupta, A.K. Chaturvedi, and R. Budhiraja, "Improved Rate-Energy Trade off for Energy Harvesting Interference Alignment Networks," *IEEE Wireless Commun. Lett.*, vol. 6, no. 3, June 2017, pp. 410–413.

[16] H. Gao, W. Ejaz, and M. Jo, "Cooperative Wireless Energy Harvesting and Spectrum Sharing in 5G Networks," *IEEE Access*, vol. 4, July 2016, pp. 3647–3658.

[17] Y. Gu and S. Aïssa, "RF-Based Energy Harvesting in Decode-and-Forward Relaying Systems: Ergodic and Outage Capacities," *IEEE Trans. Wireless Commun.*, vol. 14, no. 11, Nov. 2015, pp. 6425–6434.

[18] Y. Chen, "Energy-Harvesting AF Relaying in the Presence of Interference and Nakagami-m Fading," *IEEE Trans. Wireless Commun.*, vol. 15, no. 2, Sept. 2016, pp. 1008–1017.

[19] E. Boshkovska et al., "Practical Non-linear Energy Harvesting Model and Resource Allocation for SWIPT Systems," *IEEE Commun. Lett.*, vol. 19, no.12, Sept. 2015, pp. 2082–2085.

[20] C.R. Valenta and G.D. Durgin, "Harvesting Wireless Power: Survey of Energy-Harvester Conversion Efficiency in Far-Field, Wireless Power Transfer Systems," *IEEE Microw. Mag.*, vol. 15, no. 4, June 2014, pp. 108–120.

[21] Y. Dong, M.J. Hossain, and J. Cheng, "Performance of Wireless Powered Amplify and Forward Relaying over Nakagami-m Fading Channels with Nonlinear Energy Harvester," *IEEE Commun. Lett.*, vol. 20, no. 4, Apr. 2016, pp. 672–675.

[22] J. Zhang and G. Pan, "Outage Analysis of Wireless-Powered Relaying MIMO Systems with Non-linear Energy Harvesters and Imperfect CSI," *IEEE Access*, vol. 4, Oct. 2016, pp. 7046–7053.

[23] A.J. Goldsmith, *Wireless Communications*, New York, USA: Cambridge University Press, 2005.

[24] I.S. Gradshteyn and I.M. Ryzhik, *Table of Integrals, Series, and Products*, London, UK: Academic Press, 2007.

[25] Wolfram Research, Accessed 2017. http://functions.wolfram.com/

[26] A. Papoulis, *Probability, Random Variables, and Stochastic Processes*, New York, USA: McGraw-Hill, 1991.

Aleksandra Cvetkovic received her BS, MS, and PhD degrees in electrical engineering from the Faculty of Electronic Engineering, University of Nis, Serbia in 2001, 2007, and 2013, respectively. She has been with the Department of Telecommunications, Faculty of Electronic Engineering, University of Nis, Nis, Serbia since 2001, where she is now a teaching assistant. Her main research interests include wireless communication theory, cooperative communications, and free-space optical systems.

Vesna Blagojevic received her BS, MS, and PhD degrees in electrical engineering from the School of Electrical Engineering, University of Belgrade, Serbia in 2001, 2007, and 2014, respectively. She has been with the Department of Telecommunications, School of Electrical Engineering, University of Belgrade, since 2001, where she currently holds the position of assistant professor. Her main research interests lie in the field of wireless communication theory, cognitive radio, and cooperative communications.

Predrag Ivaniš received his BS, MS, and PhD degrees in electrical engineering from the School of Electrical Engineering, University of Belgrade, Serbia in 1999, 2004, and 2008, respectively. Since 2001, he has been with Department of Telecommunications, School of Electrical Engineering, University of Belgrade, where he is now an associate professor. His main research interests include wireless communications theory, information theory, and error control coding.